Skin Region Segmentation based on the Average Preprocessed Image of Multicolor Face Image Sequence

Wei Li[1], Xianbo He[1] & Fangyuan Jiao[1]

[1]Xiangbinxiaozhen 2qi 1-1-503 Nanchong, Sichuan, China
Email: nos036@163.com

Abstract. This paper proposes a method for skin region segmentation for face images with unbalanced color and light based on preprocessing of a multicolor face image sequence. In this method, multicolor face images from a sequence are preprocessed in order to remove color offset and uneven brightness. Then the color data from the preprocessed face images are used for taking the average in order to remove noise and smoothen the face image. Finally, skin region segmentation for the average preprocessed face image is realized based on the established ellipse skin model. Experiments have shown that this method has good performance.

Keywords: *skin region; multicolor; image sequence; preprocessing; face detection.*

1   Introduction

Skin segmentation, as a mainstream approach and important stage of face detection and recognition, has a wide range of applications, such as virtual reality, video-conferencing, intelligent human machine interfaces, security systems, etc. The efficiency of skin segmentation influences the performance of these systems. Various methods have been proposed for skin segmentation [1-11]. Among these methods, those based on skin color information or skin color model are classic [4-9]. Methods using mixed technologies are now common, such as combining color and edge detection [1], combining color and template matching [2,5], combining color and neural network [3], combining a piecewise linear decision boundary (PLDB) and Gaussian mixture models (GMM) [9]. The information of color image series can also be used to help face detection [10]. However, for a face image made under conditions of unbalanced or abnormal color and light it is still a challenge to improve the segmentation accuracy while ensuring the speed of processing.

In this paper, the color information from multicolor face image sequences is considered for face images with unbalanced or abnormal color and light. In order to decrease the influence of interference or noise and improve the average segmentation accuracy, the proposed method segments the skin targets by respective adaptive preprocessing of multicolor face images from a sequence,

taking the average of the preprocessed face images and establishing the ellipse skin model for the average preprocessed image.

2   Methodology

2.1   Process of Method

As shown in Figure 1, the process of segmentation in this method includes five procedures: input the multicolor face image sequence, preprocess the multicolor face images from the sequence, calculate the average of the preprocessed face images from the sequence, establish the ellipse skin model for the average preprocessed image, and finally segment the skin regions based on the ellipse model.
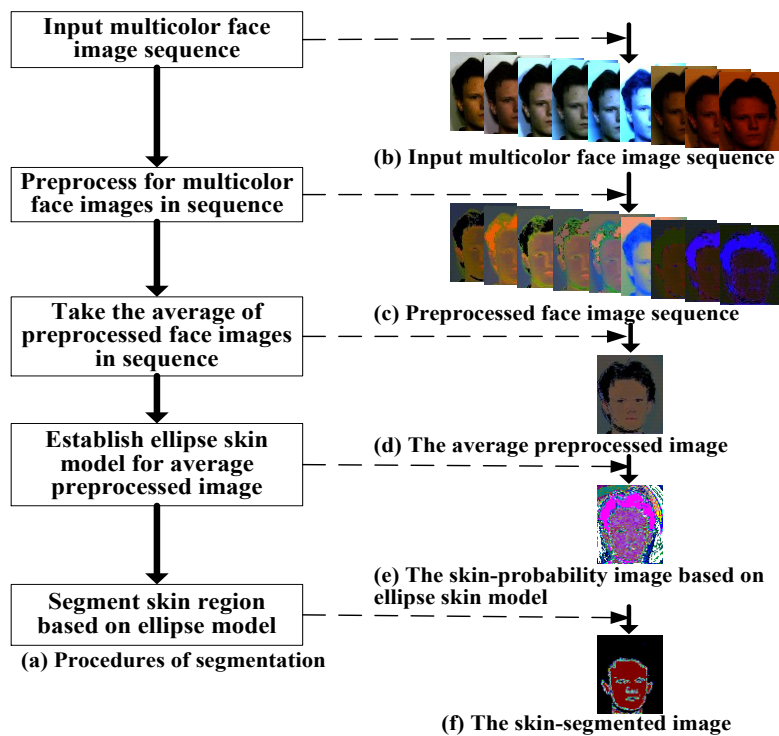

(b) Input multicolor face image sequence

(c) Preprocessed face image sequence

(d) The average preprocessed image

(e) The skin-probability image based on ellipse skin model

(f) The skin-segmented image

(a) Procedures of segmentation

Figure 1 Procedure of segmentation and the acquired images.

As shown in Figure 1(b), the first procedure is to collect multicolor face images in the form of a sequence. 'Multicolor' means that the gathered face images in the sequence have different colorcasts, which requires different color light sources. The second procedure is to balance the color and light for smoothing

the face images and reducing noise caused by unbalanced color and light. Accordingly, the acquired preprocessed face images from the sequence are shown in Figure 1(c). The third procedure is to calculate the average of the preprocessed face images from the sequence after preprocessing, through which the average preprocessed image can be acquired, as shown in Figure 1(d). In order to lay the foundation for segmentation, the fourth procedure is to establish the ellipse skin model for the average preprocessed image, based on which a skin-probability image can be acquired, as shown in Figure 1(e). The final procedure is to segment the skin targets in the skin-probability image based on the established ellipse model. By segmentation a skin-segmented image can be acquired, as shown in Figure 1(f).

2.2 Preprocessing

In order to depress the influence of unbalanced color and light, smoothen the face images and reduce noise for better distinguishing the face from the background, the preprocessing combines data from three relationships to obtain adaptive color adjustment coefficients. The three relationships consist of: the relationship between multiple components (R, G, and B) and a single component (R, or G, or B), the relationship between global information (accumulations or averages) and local information (pixel values), as well as the relationship between each other of the local information of every pixel. As shown in Figure 2, the procedure for preprocessing every face image in the sequence is as follows:
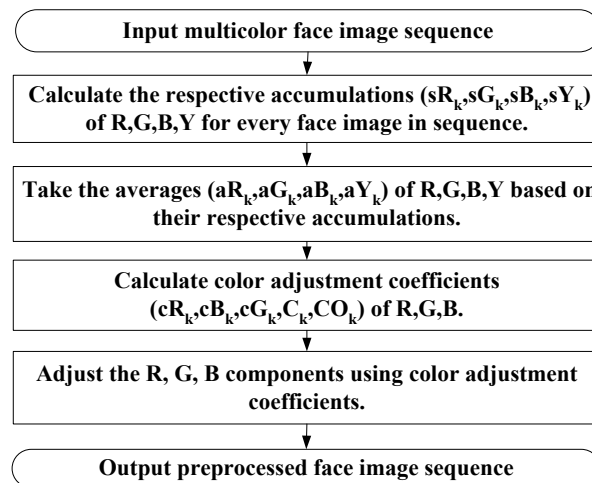

Figure 2 Procedures of preprocessing.

1. Input the multicolor face image sequence (Figure 4(a)).

2. Calculate the respective accumulations (sR_k, sG_k, sB_k, sY_k) of R,G,B,Y for every face image in the sequence by Eq. (1).

$$\begin{cases} sR_k = \sum_{j=0}^{H-1}\sum_{i=0}^{W-1} R_{k,i,j}, \, sG_k = \sum_{j=0}^{H-1}\sum_{i=0}^{W-1} G_{k,i,j}, \, sB_k = \sum_{j=0}^{H-1}\sum_{i=0}^{W-1} B_{k,i,j}, \, sY_k = \sum_{j=0}^{H-1}\sum_{i=0}^{W-1} Y_{k,i,j}, \\ Y_{k,i,j} = 0.299 \times R_{k,i,j} + 0.578 \times G_{k,i,j} + 0.114 \times B_{k,i,j} \end{cases} \quad (1)$$

where, i, j are a pixel's abscissa and ordinate, k is the serial number of the image in the sequence. $R_{k,i,j}, G_{k,i,j}, B_{k,i,j}$ are the R, G, and B components of the first k image in the input multicolor face image sequence.

3. Take the respective averages (aR_k, aG_k, aB_k, aY_k) of R,G,B,Y based on their respective accumulations by Eq. (2).

$$aR_k = \frac{sR_k}{(W \times H)}, \quad aG_k = \frac{sG_k}{(W \times H)}, \quad aB_k = \frac{sB_k}{(W \times H)}, \quad aY_k = \frac{sY_k}{(W \times H)} \quad (2)$$

where , H and W are the height and width of the image.

4. Calculate the color adjustment coefficients ($cR_k, cG_k, cB_k, C_k, CO_k$) of R,G,B based on three relationships, as shown in Eq. (3)-(5).

$$cR_k = \frac{((aR_k + aG_k + aB_k)/3)}{aR_k}, cG_k = \frac{((aR_k + aG_k + aB_k)/3)}{aG_k}, cB_k = \frac{((aR_k + aG_k + aB_k)/3)}{aB_k} \quad (3)$$

$$C_k = \left(\begin{array}{l} \arctan(\frac{R_{k,i,j}}{G_{k,i,j}}) + \arctan(\frac{R_{k,i,j}}{B_{k,i,j}}) + \arctan(\frac{G_{k,i,j}}{R_{k,i,j}}) \\ + \arctan(\frac{G_{k,i,j}}{B_{k,i,j}}) + \arctan(\frac{B_{k,i,j}}{G_{k,i,j}}) + \arctan(\frac{B_{k,i,j}}{R_{k,i,j}}) + \arctan(\frac{aY_k}{Y_{k,i,j}}) \end{array} \right) \Big/ 2\pi \quad (4)$$

$$CO_k = aY_k \big/ Y_{k,i,j} \quad (5)$$

5. Adjust the R, G, and B components using the color adjustment coefficients (cR_k, cG_k, cB_k, C_k, CO_k) by Eq. (6)-(7).

$$\begin{cases} R'_{k,i,j} = R_{k,i,j} \times cR_k \times C_k \times CO_k \\ G'_{k,i,j} = G_{k,i,j} \times cG_k \times C_k \times CO_k \\ B'_{k,i,j} = B_{k,i,j} \times cB_k \times C_k \times CO_k \end{cases} \quad (6)$$

$$\begin{cases} R'_{k,i,j} = 255 \; if(R'_{k,i,j} \geq 255), \\ G'_{k,i,j} = 255 \; if(G'_{k,i,j} \geq 255), \\ B'_{k,i,j} = 255 \; if(B'_{k,i,j} \geq 255) \end{cases} \quad (7)$$

where, $R'_{k,i,j}$, $G'_{k,i,j}$, $B'_{k,i,j}$ are the R, G, and B components of the first k image in the preprocessed face image sequence.

6. Output the preprocessed face image sequence (Figure 4(g)).

Figure 3 shows three groups of comparisons between the PDD (probability density distribution) curve of an input face image and the PDD curve of a preprocessed face image. By comparison, the two peaks of the component's (R, G, or B) PDD curve of the preprocessed face image are more sharp-pointed and obvious than those of the component's PDD curve of the input face image. This means that the face and background are easier to distinguish. Moreover, noise, color excursion, and uneven exposure have been inhibited. Thus, the preprocessing is beneficial for the subsequent modeling and segmentation.

(a)   (b)   (c)   (d)   (e)   (f)

(g)   (h)   (i)   (j)   (k)   (l)
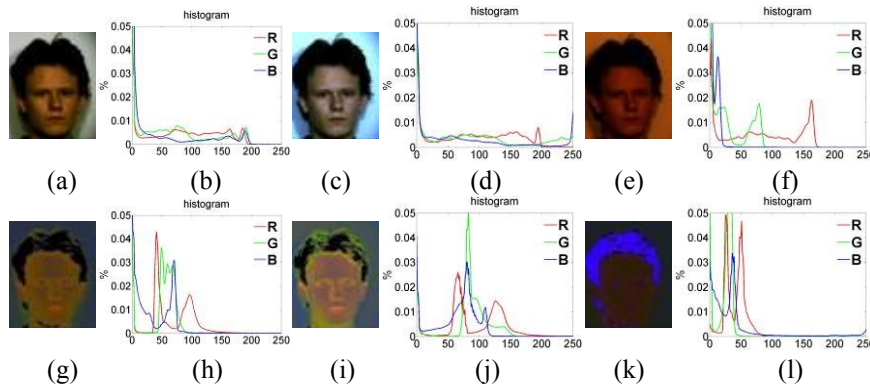
(a) Face image (No.1) in input sequence; (b) PDD curve of R,G,B of (a); (c) face image (No.3) from input sequence; (d) PDD curve of R,G,B of (c); (e) face image (No.8) from input sequence; (f) PDD curve of R,G,B of (e); (g) preprocessed face image of (a); (h) PDD curve of R,G,B of (g); (i) preprocessed face image of (c); (j) PDD curve of R,G,B of (i); (k) preprocessed face image of (e); (l) PDD curve of R,G,B of (k).

Figure 3   Images in process of segmentation.

Figure 4 shows the results of modeling and segmentation of the input face image sequence, the preprocessed face image sequence, and the sequence's average image. Comparing Figure 4(g) with 4(a), the preprocessed image in the sequence balances the color and light. Some noise was depressed. The face and the background are smoother and easier to distinguish from each other than the corresponding input face image in the sequence. Comparing Figure 4(k) with 4(e), the corresponding skin-segmented images (based on the CbCr ellipse skin model) of the preprocessed face image from the sequence have more real skin targets and less non-skin targets than those of the input face image sequence.

2.3   Taking the Average of Preprocessed Face Images

As shown in Figure 4(g), there are still some abnormal color blocks and interfering noise in the preprocessed face images. These make objects (e.g. face, hair, and background) uneven or unclear. For depressing or removing color blocks and noise this paper used the preprocessed face image sequence to take an average value as described in Eq. (8). In this way, the average preprocessed image is acquired, as shown in Figure 4(h).
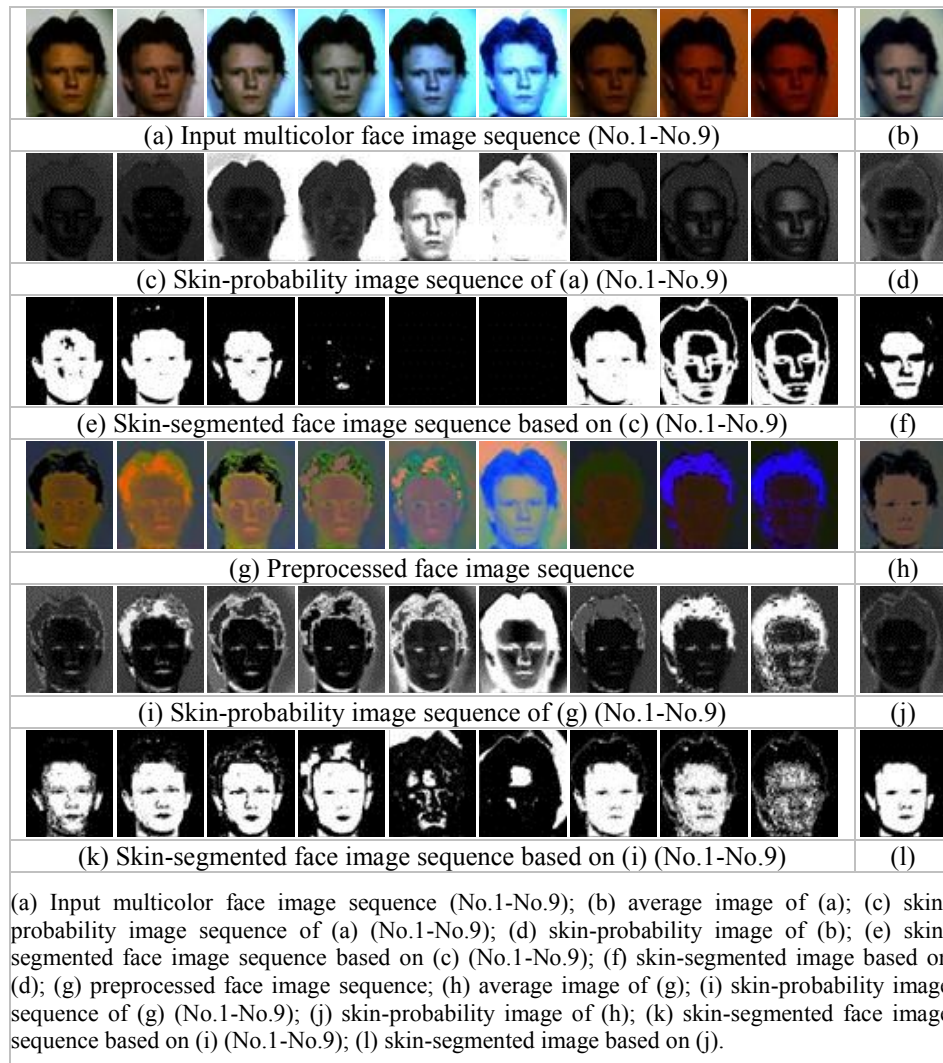

(a) Input multicolor face image sequence (No.1-No.9); (b) average image of (a); (c) skin-probability image sequence of (a) (No.1-No.9); (d) skin-probability image of (b); (e) skin-segmented face image sequence based on (c) (No.1-No.9); (f) skin-segmented image based on (d); (g) preprocessed face image sequence; (h) average image of (g); (i) skin-probability image sequence of (g) (No.1-No.9); (j) skin-probability image of (h); (k) skin-segmented face image sequence based on (i) (No.1-No.9); (l) skin-segmented image based on (j).

Figure 4 Results of modeling and segmentation for input face image sequence, preprocessed face image sequence, and sequence's average image.

$$\bar{R}_{i,j}=\frac{1}{N}\sum_{k=0}^{N-1}R'_{k,i,j}\,,\;\bar{G}_{i,j}=\frac{1}{N}\sum_{k=0}^{N-1}G'_{k,i,j}\,,\;\bar{B}_{i,j}=\frac{1}{N}\sum_{k=0}^{N-1}B'_{k,i,j} \tag{8}$$

where, i, j are a pixel's abscissa and ordinate, k is the serial number of the image in the sequence. $\bar{R}_{i,j}$, $\bar{G}_{i,j}$, $\bar{B}_{i,j}$ are a pixel's average values for the N (N=9) preprocessed face images in the sequence.

Figure 5 shows the PDD curves (Figure 5(b), 5(d), 5(f)) of three preprocessed face images (Figure 5(a), 5(c), 5(e)), the PDD curve (Figure 5(h)) of the average input face image (Figure 5(g)), and the PDD curve (Figure 5(j)) of the average preprocessed face image (Figure 5(i)).
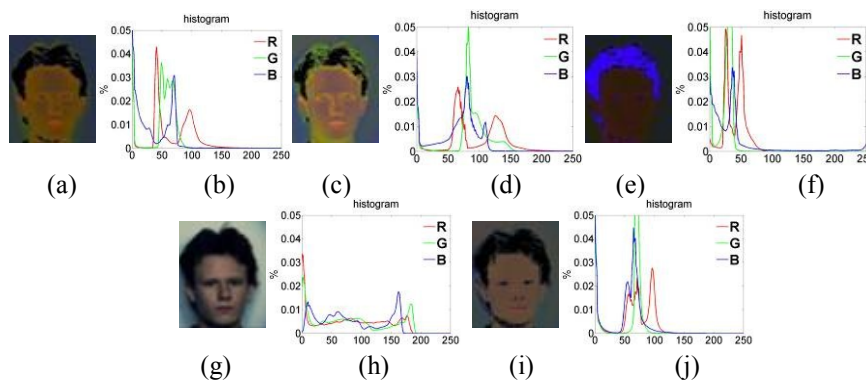
(a) Preprocessed face image (No.1) in preprocessed face image sequence; (b) PDD curve of R,G,B of (a); (c) preprocessed face image (No. 3) in preprocessed face image sequence; (d) PDD curve of R,G,B of (c); (e) preprocessed face image (No.8) in preprocessed face image sequence; (f) PDD curve of R,G,B of (e); (g) average input face image; (h) PDD curve of R,G,B of (g); (i) average preprocessed face image; (j) PDD curve of R,G,B of (i).

Figure 1　Images in process of segmentation

Note that the two peaks (Figure 5(j)) in the PDD curve of the average preprocessed face image (Figure 5(i)) are more sharp-pointed than those (Figure 5(h)) in the PDD curve of the average input face image (Figure 5(g)). Comparing Figure 4(l) with 4(f), the corresponding skin-segmented image (based on CbCr ellipse skin model) of the average preprocessed face image has less over-segmentation and under-segmentation than that of the average input face image. This also indicates that preprocessing helped to better distinguish the face from the background. Otherwise, by comparison and analysis, the PDD curve (Figure 5(j)) of the average preprocessed face image (Figure 5(i)) kept the feature of two sharp-pointed peaks but had more balanced relationships between the three color components than the PDD curves (Figure 5(b), 5(d), 5(f)) of the three preprocessed face images (Figure 5(a), 5(c), 5(e)). This means that by

taking the average, the face and the background in the average preprocessed face image are still easy to distinguish, but color excursion, uneven exposure and noise have been inhibited further. Contrasting Figure 4(h) and 4(g), the difference between the face and the background in the average preprocessed face image is more explicit than in each preprocessed face image, because abnormal color blocks and interfering noise have obviously decreased. Comparing Figure 4(l) with 4(k), the skin-segmented image (based on the CbCr ellipse skin model) of the average preprocessed face image has less over-segmentation and under-segmentation than the skin-segmented preprocessed face images. Therefore, the average technology for the preprocessed face image is also beneficial for the subsequent modeling and segmentation.

2.4   Skin Region Segmentation based on Skin Color Model

The purpose of skin segmentation is to partition a face image into skin regions. For the problem of face recognition, segmentation can remove non-skin regions in order to help reduce search scope and identify probable face targets. Although there are many different methods of skin segmentation, in this paper segmentation based on a skin color model is considered. In several classical skin models [4-6] (e.g. the Gaussian mixture model and the ellipse model), the CbCr ellipse skin model is adopted. Figure 6 shows the procedures of skin segmentation based on the CbCr ellipse skin model.
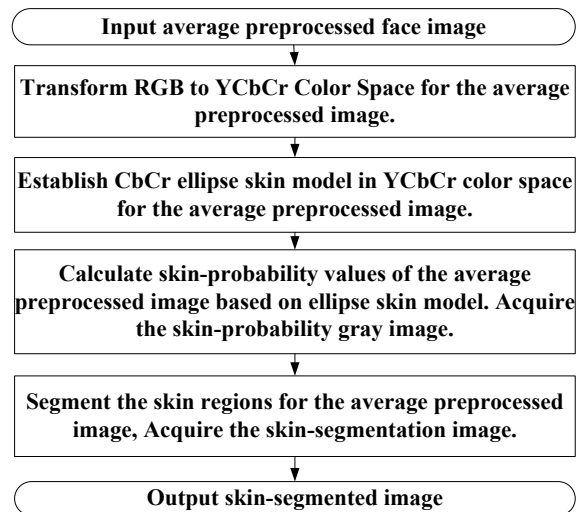

Figure 2 Procedures of skin segmentation

As shown in Figure 6, the procedures of skin segmentation, based on an established ellipse model, are described as follows:

1. Input the average preprocessed face image (Figure 4(h)).
2. Transform *RGB* to *YCbCr* color space for the average preprocessed image according to Eq. (9).

$$\begin{bmatrix} Y_{i,j} \\ Cr_{i,j} \\ Cb_{i,j} \end{bmatrix} = \begin{bmatrix} 0.299 & 0.587 & 0.114 \\ 0.500 & -0.4187 & -0.0813 \\ 0.1687 & -0.3313 & 0.500 \end{bmatrix} \begin{bmatrix} \bar{R}_{i,j} \\ \bar{G}_{i,j} \\ \bar{B}_{i,j} \end{bmatrix} + 128 \tag{9}$$

3. Establish the ellipse skin model in *YCbCr* color space for the average preprocessed image by Eq. (10).

$$\begin{bmatrix} x \\ y \end{bmatrix} = \begin{bmatrix} \cos\theta & \sin\theta \\ -\sin\theta & \cos\theta \end{bmatrix} \begin{bmatrix} Cb_{i,j} - C_x \\ Cr_{i,j} - C_y \end{bmatrix}, \quad \frac{(x - eC_x)}{a^2} + \frac{(y - eC_y)}{b^2} \le 1 \tag{10}$$

$$P_{i,j} = \frac{(x - eC_x)}{a^2} + \frac{(y - eC_y)}{b^2} \tag{11}$$

where, $C_x = 109.38$, $C_y = 152.2$, $\theta = 2.53$, $eC_x = 1.60$, $eC_y = 2.41$, $a = 25.39$, $b = 14.03$. These parameters are computed from the skin cluster in CbCr color space.

4. Calculate the skin-probability values ($P_{i,j}$) of the average preprocessed image based on the ellipse model by Eq. (11). Acquire the skin-probability gray image (Figure 4(j)) by Eq. (12), using a skin-probability value.

$$T_{i,j} = \begin{cases} P_{i,j} \times 0.01 \times 255 & else \\ 255 & if (P_{i,j} \ge 10) \end{cases} \tag{12}$$

where, $T_{i,j}$ is the gray value of the skin-probability gray image.

5. Segment the skin regions of the average preprocessed image by Eq. (13) based on which skin-segmentation image can be acquired (Figure 4(l)).

$$S_{i,j} = \begin{cases} 255 & if (P_{i,j} < 1) \\ 0 & else \end{cases} \tag{13}$$

where, $S_{i,j}$ is skin-segmented image.

6. Output the skin-segmented image (Figure 4(k)).

Figures 4(c), 4(d), 4(i), and 4(j) show the acquired skin-probability images based on the ellipse skin model that were respectively built from the input multicolor face image sequence (Figure 4(a)), the average input face image (Figure 4(b)), the preprocessed face image sequence (Figure 4(g)), and the average preprocessed face image (Figure 4(h)). Comparing Figure 4(j) with 4(c), 4(d), and 4(i), it is clear that the skin-probability image of the average preprocessed face image describes and reflects the distribution of the skin

targets better and more evenly. Respectively corresponding to Figures 4(c), 4(d), 4(i), 4(j), the Figs. 4(e), 4(f), 4(k), 4(l) show the acquired skin-segmented images based on the ellipse skin model. Comparing Figure 4(l) with 4(e), 4(f), and 4(k), the skin-segmented image of the average preprocessed face image has the best segmentation effect because of the combined use of the preprocessing and the average technology.

3 Results and Discussion

The performance of the proposed algorithm was evaluated with a self-built face image sequence test set, which came from the University of Oulu physics-based face database [12] and AUTODYN. The self-built face image sequence test set contained 20 sequences (180 faces) with different color casts and light conditions. The test environment was: P4 + 2GHz CPU + WinXP + VC6 + MATLAB 7.0. In the test, every input face image sequence contained at least three kinds of color light sources. All the input face images in the sequence were approximately resized to a normalized size of 50×60 pixels for processing. The range of time-consumption in each stage of the proposed method is listed in Table 1. From Table 1, it can be seen that the segmentation method proposed in this paper has a satisfactory speed. Table 2 lists a comparison between the average segmentation correct rate (ASCR) and average segmentation error rate (ASER) of four methods. The ASCR is defined as the ratio of area of correctly segmented skin regions to the total area of skin regions in all images. The ASER is defined as the ratio of area of falsely segmented skin regions to the total area of skin regions in all images. From Table 2 it can be seen that the proposed segmentation method, which is based on the CbCr ellipse model for an average preprocessed face image, has a higher average segmentation correct rate and lower average segmentation error rate than the other methods.

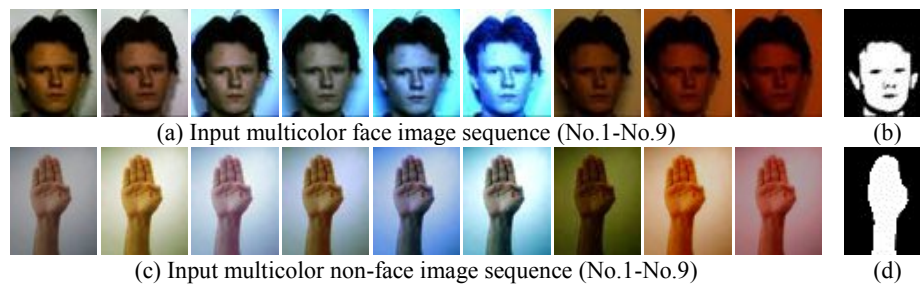**Table 1**   Time-consumption in each stage of proposed method.

Stages	Time-consumption (ms)	Normalized size (Pixels)
Input + preprocessing	94~100	50×60
Take the average	0~15	50×60
Acquire the skin-probability	0~5	50×60
Skin segmentation	0~5	50×60
Total	**94~125**	**50×60**

This study mainly focused on skin segmentation using color information and a skin model. It didn't classify face objects and non-face objects with the same characteristics as face color. When segmenting skin regions, sometimes some non-face objects (such as hands, arms, legs) with the same characteristics as

face color are also segmented, as shown in Figure 7(d). However, all the segmented skin regions (face objects and non-face objects) can be regarded as

Table 2   The ASCR and ASER of four segmentation methods.

Segmentation Methods	Method 1[1] [6,7]	Method 2[2]	Method 3[3]	Method 4[4] [2, 5]	Method 5[5]
ASCR (%)	53.8	66.2	72.6	93.2	97.9
ASER (%)	37.5	32.8	29.3	8.7	7.6
No. of faces	180	180	180	180	180

(a) Input multicolor face image sequence (No.1-No.9)   (b)

(c) Input multicolor non-face image sequence (No.1-No.9)   (d)

(a) Input multicolor face image sequence (No.1-No.9); (b) skin-segmented image of (a) using proposed method; (c) input multicolor non-face image sequence (No.1-No.9); (d) skin-segmented image of (c) using proposed method.

Figure 3 Results of Segmentation for Input Face Image Sequence and non-face Image Sequence.

(a)   (b)   (c)   (d)   (e)   (f)   (g)   (h)   (i)
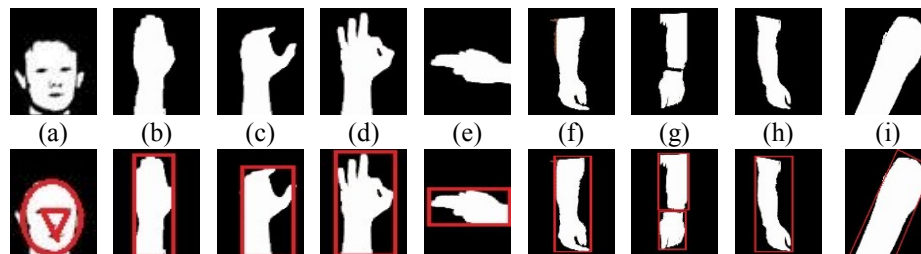
(a) Face object; (b) non-face object (No.1); (c) non-face object (No.2); (d) non-face object (No.3); (e) non-face object (No.4); (f) non-face object (No.5); (g) non-face object (No.6); (h) non-face object (No.7); (i) non-face object (No.8).

Figure 4 The face candidate targets.

---

[1] Segmentation based on CbCr ellipse skin model built for input multicolor face image sequence.

[2] Segmentation based on CbCr ellipse skin model built for average input multicolor face image sequence.

[3] Segmentation based on CbCr ellipse skin model built for preprocessed face image sequence.

[4] Segmentation based on GMM model built for input multicolor face image sequence.

[5] Segmentation based on CbCr ellipse skin model built for average preprocessed image.

face candidate targets in subsequent face classification stages. The face candidate targets will be classified by combining the information of the targets' geometrical shape and internal holes, as shown in Figure 8.

4   Conclusions

In this paper a skin region segmentation method based on an average preprocessed face image was proposed. In this method, the adaptive preprocessing technology is used for each respective face image in the sequence to reduce abnormal color blocks and some noise, while the average technology is used to confuse the information of the multicolor face images in the sequence. As exhibited in the experiments, the final outcome of this study was a skin-segmented single facial image. Experiments demonstrated that the proposed method had a good performance and can be applied for single-face recognition or detection. This method may be applied to multiple-face recognition or detection in a following work. One drawback of the proposed method is that it requires a specific input environment, especially the different color light sources. In order to collect rich information of facial skin color for achieving a good skin segmentation result, it is best that the multicolor face images in the input sequence have the same pose, at least three kinds of colorcast and at least three kinds of exposure levels. Therefore at least three exposure levels (overexposure, normal exposure, and underexposure) and at least three color light sources (red, blue, yellow or green) should be adopted to make nine multicolor input images with the same pose.

References

[1]   Vijay Lakshmi, H.C. & Patil Kulakarni, S., *Segmentation Algorithm for Multiple Face Detection in Color Images with Skin Tone Regions using Color Spaces and Edge Detection Techniques*, International Journal of Computer Theory and Engineering, **2**(4), pp. 552-558, 2010.
[2]   Tripathi S., Sharma V. & Sharma S., *Face Detection using Combined Skin Color Detector and Template Matching Method*, International Journal of Computer Applications, **26**(7), pp. 5-8, 2011.

[3]   Wang Z.J. & Li, A.T., *Face Detection Based on Skin Color and Neural Network*, 2008 International Conference on Computer Science and Software Engineering, Wuhan, China, pp. 961-964, Dec. 2008.

[4]   Shih, F.Y., Cheng, S.X. & Chuang, C.F., *Extracting faces and facial features from color images*, International Journal of Pattern Recognition and Artificial Intelligence, **22**(3), pp. 515-534, 2008.

[5]   Wang, Z.W. & Li, S.Z., *Face Recognition using Skin Color Segmentation and Template Matching*, Information Technology Journal, **10**, pp. 2308-2314, 2011.

[6]   Hsu, R.L., Abdel-Mottaleb, M. & Jain, A.K., *Face Detection in Color Images*, IEEE Trans. Patter. Anal. and Mach. Intell., **24**(5), pp. 25-29, May 2002.

[7]   Zhang, D.Z., Wu, B.Y., Sun, J.B. & Liao, Q.L., *A Face Detection Method Based on Skin Color Model*, In Proceeding of the 11th joint Conference on Information Science, December, 2008.

[8]   Sagheer A. & Aly S., *An Effective Face Detection Algorithm Based on Skin Color Information*, 2012 Eighth International Conference on Signal Image Technology and Internet Based Systems (SITIS), pp. 90-96, Nov. 2012.

[9]   Hadi, S., Ahmad, A.S., Suwardi, I.S. & Wazd, F., *DEWA: A Multiaspect Approach for Multiple Face Detection in Complex Scene Digital Image*, ITB J. ICT, **1C**(1), pp. 16-28, 2007.

[10]   Yang J., Ling X.F., Zhu Y.T. & Zheng, Z.I., *A Face Detection and Recognition System In Color Image Series*, Mathematics and Computers in Simulation, **77**, pp. 531-539, 2008.

[11]   Ibrahim, N.B., Selim, M.M. & Zayed, H.H., *A Dynamic Skin Detector Based on Face Skin Tone Color*, Proceedings of 2012 8th International Conference on Informatics and Systems, pp. MM-1-MM-5, 2012.

[12]   http://www.cse.oulu.fi/CMV/Downloads/Pbfd#Example:_person_9 4 (5 July 2013).